ELSEVIER

Solid State Ionics 86–88 (1996) 897–902

SOLID STATE IONICS

Dynamically compacted rechargeable ceramic lithium batteries

M.J.G. Jak*, E.M. Kelder, M. Stuivinga, J. Schoonman

Delft University of Technology, Laboratory for Applied Inorganic Chemistry, Julianalaan 136, 2628 BL Delft, Netherlands

Abstract

A rechargeable ceramic battery is made of a $Li_xMn_2O_4$ ($x = 1.1$) cathode, a graphite anode and a BPO_4:yLi_2O ($y \simeq 0.035$) solid electrolyte by dynamic compaction. This battery system has a theoretical open-circuit potential of 4.2 V and a high energy density, which makes it interesting for application in electric vehicles.

Keywords: Lithium battery; Ceramic battery; Energy density; Dynamic compaction

1. Introduction

This paper deals with the synthesis and characterisation of the starting materials $Li_xMn_2O_4$ ($x = 1.1$) and BPO_4:yLi_2O ($y \simeq 0.035$), and the compaction behaviour of these materials.

In order to manufacture high capacity, all-solid-state ceramic lithium batteries, conventional methods are inadequate. The usual problem of ceramic batteries is the high internal resistance, caused by both the solid electrolyte and the interfaces between the different cell components. With dynamic compaction, the interfaces are pressed together with very high forces, therefore, increasing the contact area and decreasing the interfacial resistances. Optimal battery components require the use of powders with specific properties, like homogeneity, small (preferably submicron) grain sizes, as well as a narrow size distribution.

The mixed ionic–electronic conductor (MIEC), $Li_xMn_2O_4$, is used as the cathode material. Here, $Li_xMn_2O_4$ with $x = 1.1$ was selected, because in the first charging step, approximately 20 mol% of Li will remain irreversibly in the carbon anode [1]. From Fig. 1 it is clear that x-values smaller than 1.0 are desired in order to obtain the highest voltage. The open cell voltage (OCV) is equal to the potential difference between $Li_xMn_2O_4$ and C_6Li_z.

As the lithium ion conducting solid electrolyte, lithium-doped boron phosphate, BPO_4:yLi_2O ($0.0 < y < 0.15$) was used. This solid electrolyte, as well as the cathode material, is synthesized using readily available precursor compounds. BPO_4:yLi_2O with $y = 0.035$ is used as the solid electrolyte material in the battery. This material with 7 mol% Li exhibits a maximum in the conductivity-composition isotherm [2].

A.C.-impedance spectroscopy is used to determine the electrical properties of the starting materials. Important properties of the battery components are bulk and grain boundary electrical conductivities. In order to investigate the relation between dynamic compaction and the resulting micro- and macrostructure, the cathode and electrolyte materials are compacted separately. Because there are no dynamic compaction data (so called Hugoniot) of these ma-

*Corresponding author.

PII S0167-2738(96)00205-6

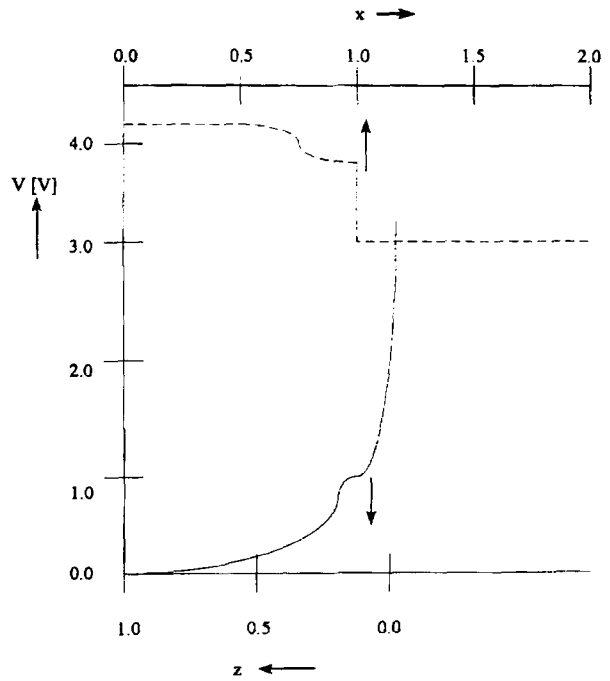

Fig. 1. Open cell voltage as a function of x in $Li_xMn_2O_4$ [3] and z in Li_zC_6 [1].

terials available, different parameters are varied in order to obtain the optimum compaction of these materials. Finally, a complete battery was manufactured using dynamic compaction.

2. Experimental

2.1.1. Synthesis of $Li_{1.1}Mn_2O_4$.

$Li_{1.1}Mn_2O_4$ is synthesized using a wet chemical technique. Well-defined powders are obtained by reacting manganese acetate and lithium hydroxide. A calcining step of 600°C is used to oxidize the precursors [3,4]. The theoretical maximum density (TMD) is 4.436 g/cm^3, determined with XRD measurements. Furthermore, XRD measurements reveal that the synthesized $Li_{1.1}Mn_2O_4$ is crystalline with the spinel structure and single phase. The $Li_{1.1}Mn_2O_4$ powder, as synthesized, has an average grain size of 20 μm. Ball milling (using a Frisch planetary micromill Pulverisette 7) reduces the grain size down to 1 μm. Pellets of ball milled $Li_{1.1}Mn_2O_4$ were made by uniaxially pressing mixtures of powders of $Li_{1.1}Mn_2O_4$ with 10 wt.% PTFE with approximately 30 MPa. The pellets have a diameter of 10.0 mm and a thickness of approximately 1.5 mm. The pellets are mounted between two aluminium electrodes and the impedance spectra are measured with a Schlumberger Solartron 1260 Frequency Response Analyzer. The applied voltage is 20 mV in the frequency range of 10 Hz to 1 MHz. The temperature is varied between 278 and 333 K. This temperature range is chosen because of the application of this material as the cathode material in rechargeable batteries with operating temperatures of around room temperature.

2.1.2. Synthesis of BPO_4:0.035Li_2O

BPO_4:0.035Li_2O is synthesized using equimolar amounts of boric acid (H_3BO_3) and phosphoric acid (H_3PO_4), mixed in water. To the white paste formed, certain amounts of $LiOH.H_2O$ were added. A substantial amount of lithium can be dissolved into the BPO_4 lattice, rendering solid solutions of BPO_4:yLi_2O, a lithium ion conducting electrolyte.

Several drops of the paste was used to form a uniform layer between two carbon platelets (15 × 15 mm). The samples were heated in air using a programmable furnace (NEY 2-525 series II) using the following temperature program:

heating from room temperature to 110°C at a rate of 2°C/min,

keeping the samples for 2 h at 110°C,

heating from 100°C to 500°C at a rate of 4°C/min,

keeping the samples for 6 h at 500°C (the reaction temperature).

Subsequently, the samples were allowed to cool down in the furnace to room temperature. The average grain size of the powders is 2 μm. The theoretical maximum density is 2.802 g/cm^3, determined with XRD measurements. XRD analysis reveals the BPO_4:0.035Li_2O to be single phase and to have the cristobalite structure. The thickness of the BPO_4:0.035Li_2O layers turned out to be about 0.5 mm.

Impedance spectroscopy measurements were performed on these samples, using the carbon platelets as electrodes, which show good contact with the electrolyte after firing. The impedance measurements were executed with the Schlumberger Solartron 1260 Frequency Response Analyzer. The applied voltage amplitude is 100 mV and the frequency ranges from

0.01 Hz to 30 MHz. The measurements are performed between 298 and 673 K.

2.1.3. Dynamic compaction of the battery components

In a series of dynamic compaction experiments of the separate battery components, the parameters varied are the explosives (detonation velocity from 1.8 km/s to 8.0 km/s and the related pressure from 1.0 to 16 GPa), the powder container material and the plug materials (combinations of Al, Fe and stainless steel). The compactions are performed using the cylindrical configuration [5], with powder containers with an internal diameter of 9.5 mm and a length of 14.0 cm (Fig. 2). The materials are precompacted in the cylinder using tapping and uniaxial pressing with 20 MPa. Wood, steel and rubber plates are applied to absorb the shock wave at the bottom.

2.1.4. Dynamic compaction of a cylindrical battery $C/BPO_4{:}0.035Li_2O/Li_{1.1}Mn_2O_4$

As previously reported [6], the occurring pressure in the powder to be compacted, is often at its highest in the centre of the cylinder. Since the pressure necessary to compact the $BPO_4{:}0.035Li_2O$ is higher than for the $Li_{1.1}Mn_2O_4$, we chose to compact a co-axial battery, with $Li_{1.1}Mn_2O_4$ (cathode) as the outer cylinder, a $BPO_4{:}0.035Li_2O$ (electrolyte) as the inner cyclinder and with a carbon rod (anode) in the centre. The powder container is filled using different moulds, in which the powders are fit and pressed.

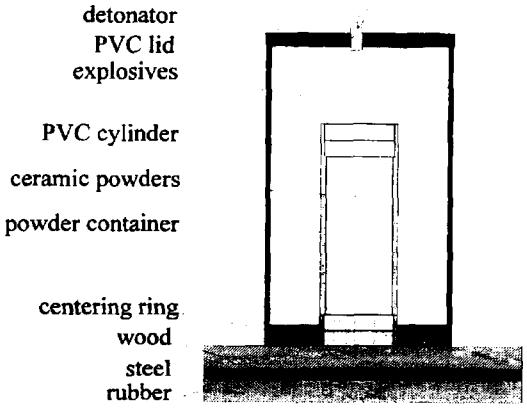

Fig. 2. Experimental set-up for dynamic compaction.

3. Results and discussion

3.1.1. A.C.-impedance spectrocopy measurements on $Li_{1.1}Mn_2O_4$

In Fig. 3a–c, three representative spectra are depicted. The spectra were fitted using the data analysis program EQUIVCRT [7]. The equivalent circuit we derived is presented in Fig. 4.

For both the electrons and the ions, the conductivity path is through bulk and grain boundaries, whereas the additional Q-element in the ionic path represents the diffusion of the lithium ions through the $Li_{1.1}Mn_2O_4$.

Excellent fits are obtained by using this equivalent circuit in the entire frequency range and are shown for all temperatures in Fig. 3. The electronic bulk and grain boundary conductivities as well as the ionic bulk and grain boundary conductivities are plotted as a function of the inverse temperature in Fig. 5a–b, respectively.

The activation energies of the bulk and grain boundary electronic and ionic conductivities are determined from the slopes of the graphs in Fig. 5a–b. The activation energy for the electronic bulk conductivity is 0.05 eV and of the electronic grain boundary conductivity is 0.39 eV. The activation energies for bulk and grain boundary ionic conductivity are 0.21 and 0.42 eV, respectively.

3.1.2. A.C.-impedance spectroscopy of $BPO_4{:}0.035Li_2O$

The overall ionic resistivity of the cell $C|BPO_4{:}0.035Li_2O|C$ is taken from the intercept of the Warburg impedance with the real axis. Fig. 6 shows the Arrhenius plot of the experimental total ionic conductivities of a sample with $y = 0.05$. The activation energy is found to be 0.3 eV and appears to be almost independent of the lithium content, y. The maximum room temperature conductivity is found to be $2 \cdot 10^{-6}$ S/cm for $y = 0.035$, with an activation energy of about 0.3 eV.

3.1.3. Dynamic compaction of $Li_{1.1}Mn_2O_4$

The compaction experiments reveal that densities up to 95% TMD can be achieved. The samples show many cracks if the density is larger than 85% TMD. Samples below 85% TMD do not show cracks. The cross section of the compacted samples with "low"

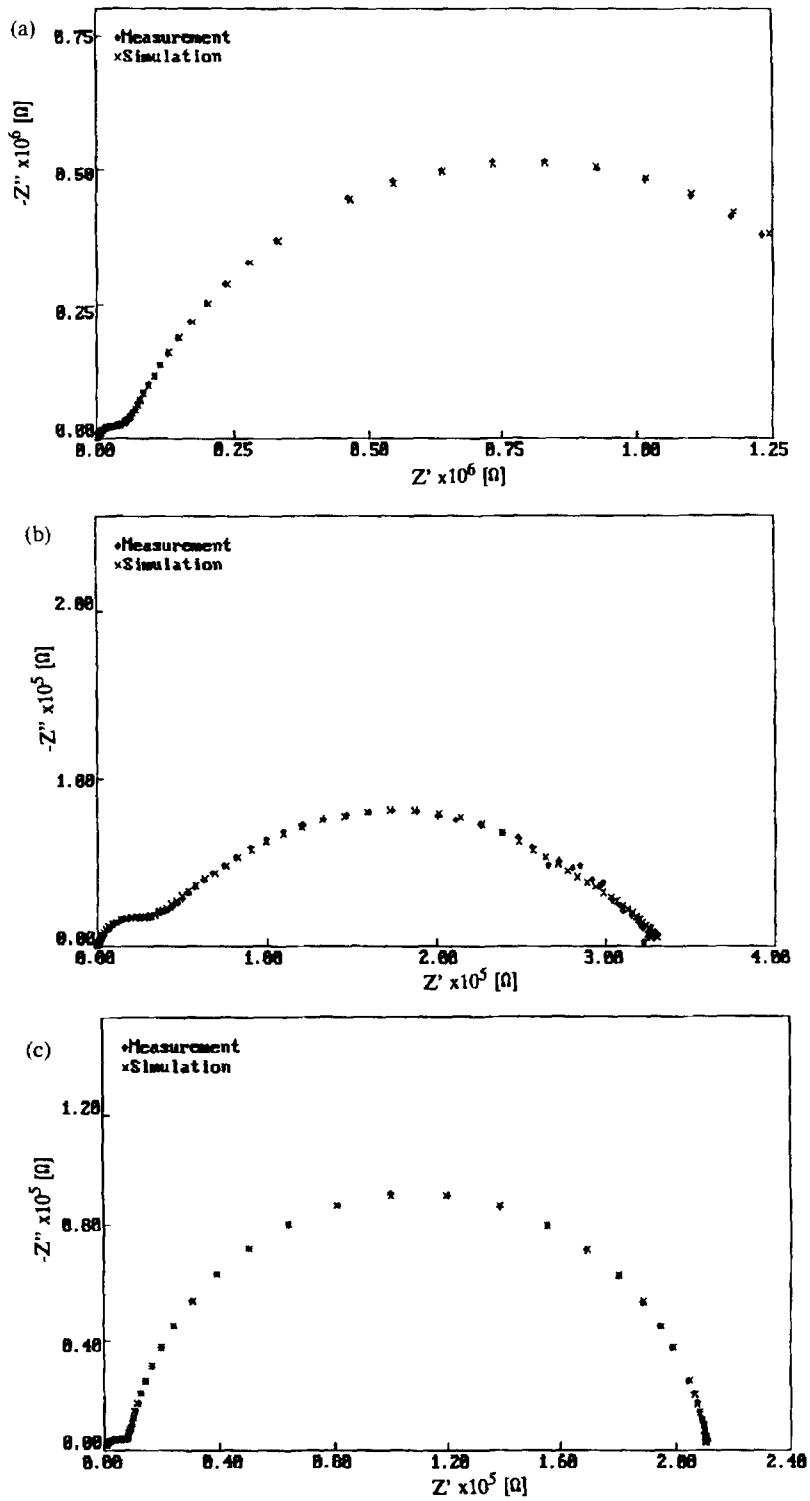

Fig. 3. A.C.-impedance spectra of $Li_{1.1}Mn_2O_4$, 10 Hz–1 MHz. (a) 298 K, (b) 296 K, (c) 326 K.

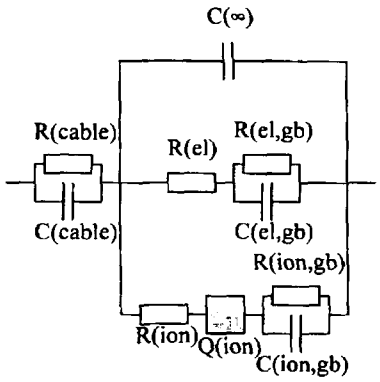

R(cable):	resistance of cables and connections
C(cable):	capacitance of cables and connections
C(∞):	geometric capacitance
R(el):	electronic bulk resistance
R(el,gb):	electronic grain boundary resistance
C(el,gb):	electronic grain boundary capacitance
R(ion):	ionic bulk resistance
Q(ion):	Warburg impedance
R(ion,gb):	ionic grain boundary resistance
C(ion,gb):	ionic grain boundary capacitance

Fig. 4. Equivalent circuit used to fit A.C.-impedance spectra of $Li_{1.1}Mn_2O_4$.

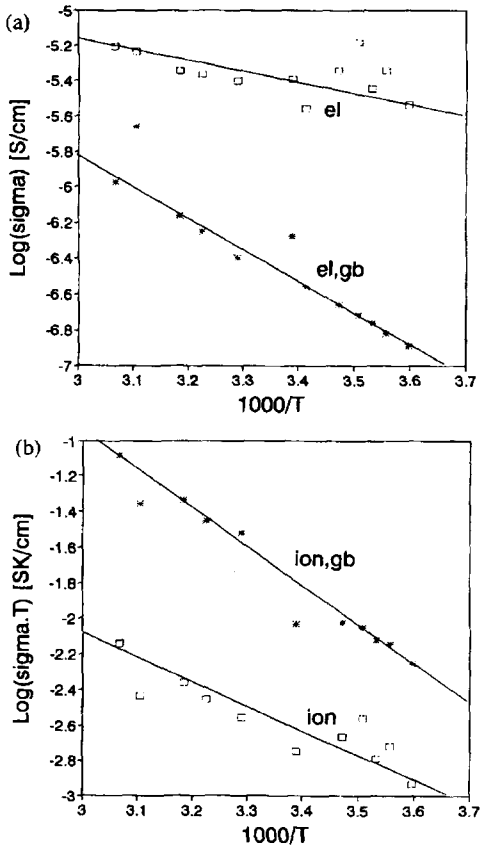

Fig. 5. Arrhenius plots $Li_{1.1}Mn_2O_4$ (a) σ_{el} and $\sigma_{el,gb}$, (b) σ_{ion} and $\sigma_{ion,gb}$.

density, show a very homogeneous densification, while the initial grains are still visible. Despite this microstructure, the densified samples show a good mechanical strength.

XRD measurements show no phase transitions nor second phases to be present after the compaction process. The XRD spectra of the samples with high density (> 85% TMD) reveal peak broadening with respect to the starting powder, indicating that defects and/or submicron grains were created during compaction.

3.1.4. Dynamic compaction of BPO_4:0.035Li_2O

The compaction experiments result in a maximum density of only 76% TMD. These densities are obtained by using explosives with a higher detonation volocity than used in the $Li_{1.1}Mn_2O_4$ compaction experiments. The samples with a higher density show cracks.

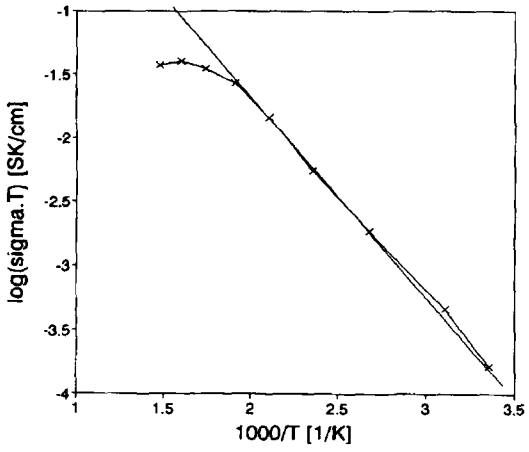

Fig. 6. Arrhenius plot of the temperature dependence of the total σ_{ion} of BPO_4:0.05Li_2O.

3.1.5. Dynamic compaction of the battery

After compaction, the $Li_{1.1}Mn_2O_4$ cylinder shows cracks due to the difference in initial density of the three different materials (Fig. 7).

SEM analysis shows a quite homogeneous compaction of the BPO_4:0.035Li_2O, except for some small cracks at the carbon side. The diameter of the carbon rod also decreased, and a homogeneous compaction is visible. SEM and backscattering microscopy show that both the interfaces $Li_{1.1}Mn_2O_4|BPO_4$:0.035Li_2O and BPO_4:0.035$Li_2O|C$ are very sharp and no mixing or reaction of materials is observed. Due to differences in initial density, high shear stresses can occur at the interfaces. Because of these shear stresses, porosities occur at some parts of the interface $Li_{1.1}Mn_2O_4|BPO_4$:0.035Li_2O. Other parts of the interface, however, are very tightly connected.

3.1.6. Electrical measurements of the cylindrical battery C/BPO_4:0.035$Li_2O/Li_{1.1}Mn_2O_4$.

Because of the relative electrolyte, the charging time is relatively long. After charging the battery for a few days with 30 V, an open circuit voltage of about 2.6 V is achieved. Possibly, this is attributed to the potential difference of the 3.9 V plateau of $Li_xMn_2O_4$ and the small plateau around 1 V plateau of Li_zC_6 (Fig. 1) [1]. Note that x and z are correlated if the molar ratio of the anode and cathode is known. The potentials are given versus Li/Li^+.

Fig. 7. Cross section of a rechargeable ceramic lithium battery, produced by dynamic compaction.

4. Conclusions

The electrical conductivities of the starting materials for the rechargeable ceramic lithium battery are summarized below:

T (K)	Conductivity of $Li_{1.1}Mn_2O_4$ [S/cm]				Conductivity of BPO_4:0.05Li_2O [S/cm] ion, total
	ion	ion, gb	el	el, gb	
278	$4.2e^{-6}$	$2.0e^{-5}$	$2.9e^{-6}$	$1.3e^{-7}$	$2.9e^{-7}$
326	$2.2e^{-5}$	$2.5e^{-4}$	$6.2e^{-6}$	$1.1e^{-6}$	$1.1e^{-4}$

Acknowledgments

The authors would like to thank Mr. F. de Lange for synthesizing BPO_4-Li_2O and XRD analysis, J.P. Lusse and A.M den Bouw for their assistance with the dynamic compaction experiments and W. Duvalois and M. Schrader for their SEM and XRD work.The Foundation for Chemical Research in the Netherlands (SON) under the Netherlands Organization for Scientific Research (NWO) is acknowledged for its financial support.

References

[1] J.R. Dahn, A.K. Sleigh, Hang Shi, B.M. Way, W.J. Weydanz, J.N. Reimers, Q. Zhong and U. von Sacken, in: Lithium Batteries, ed. G. Pistoia (1994) Ch. 1.
[2] E.M. Kelder, M.J.G. Jak, F. de Lange and J. Schoonman, Electronic Conference on Solid Electrolytes (1995).
[3] T. Ohzuku, M. Kitagawa and T.-J. Hirai, Electrochem. Soc. 137 (1990) 769.
[4] E.M. Kelder, L. Chen, X. Huang and J. Schoonman, 36th Power Sources Conference (1994) p. 114.
[5] R. Prümmer, Explosivverdichtung Pulvriger Substanzen (1987).
[6] P. Boogerd, Dynamic Compaction of Ceramics (Thesis), Delft University of Technology (1995).
[7] B.A. Boukamp, Solid State Ionics 18–19 (1986) 136.